# Analyst

Accepted Manuscript

This article can be cited before page numbers have been issued, to do this please use: S. Sathish, S. Ricoult , K. Toda-Peters and A. Q. Shen, *Analyst*, 2017, DOI: 10.1039/C7AN00273D.

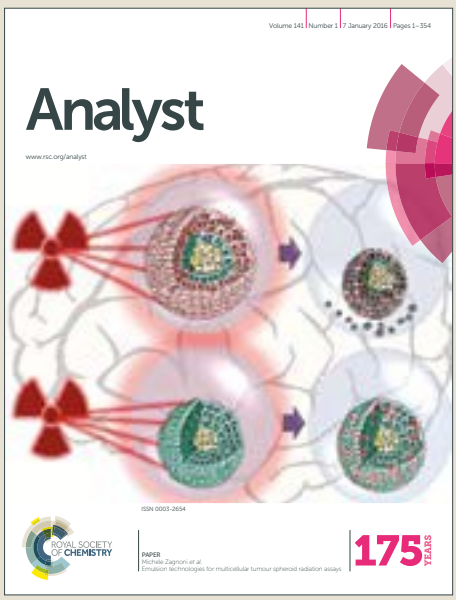




ROYAL SOCIETY OF CHEMISTRY

rsc.li/analyst

View Article Online
DOI: 10.1039/C7AN00273D
ROYAL SOCIETY OF CHEMISTRY

Journal Name

ARTICLE TYPE

Cite this: DOI: 10.1039/xxxxxxxxxx

# Microcontact printing with aminosilanes: creating biomolecule micro- and nanoarrays for multiplexed microfluidic bioassays †

Shivani Sathish,[a‡] Sébastien G. Ricoult,[a‡] Kazumi Toda-Peters[a] and Amy Q. Shen[a*]

Received Date
Accepted Date

DOI: 10.1039/xxxxxxxxxx

www.rsc.org/journalname

Microfluidic systems integrated with protein and DNA micro- and nanoarrays have been the most sought-after technologies to satisfy the growing demand for high-throughput disease diagnostics. As the sensitivity of these systems relies on the bio-functionalities of the patterned recognition biomolecules, the primary concern has been to develop simple technologies that enable biomolecule immobilization within microfluidic devices whilst preserving bio-functionalities. To address this concern, we introduce a two-step patterning approach to create micro- and nanoarrays of biomolecules within microfluidic devices. First, we introduce a simple aqueous based microcontact printing ($\mu$CP) method to pattern arrays of (3-aminopropyl)triethoxysilane (APTES) on glass substrates, with feature sizes ranging from a few hundred microns down to 200 nm (for the first time). Next, these substrates are integrated with microfluidic channels, to then covalently couple DNA aptamers and antibodies with the micro- and nanopatterned APTES. As these biomolecules are covalently tethered to the device substrates, the resulting bonds enable them to withstand the high shear stresses originated from the flow in these devices. We further demonstrated the flexibility of this technique, by immobilizing multiple proteins onto these APTES-patterned substrates using liquid-dispensing robots to create multiple microarrays. Next, to validate the functionalities of these microfluidic biomolecule microarrays, we perform (i) aptamer-based sandwich immunoassays to detect human interleukin 6 (IL6); and (ii) antibody-based sandwich immunoassays to detect human c-reactive protein (hCRP) with the limit of detection at 4 nM, a level below the range required for clinical screening. Lastly, the shelf-life potential of these ready-to-use microfluidic microarray devices is validated by effectively functionalizing the patterns with biomolecules up to 3 months post-printing. In summary, with a single printing step, this aminosilane patterning technique enables the creation of functional microfluidic micro- and nano biomolecule arrays, laying the foundation for high-throughput multiplexed bioassays.

## 1 Introduction

Since the early 1980's, microfluidic systems have advanced significantly to satisfy the growing demand for the miniaturization of bioassay devices, with applications ranging from disease diagnostics[1–4] to cell behavior studies[5–8]. Here, the main goal has been to provide cheaper, simpler and more reliable means for simultaneous detection of multiple biomarkers, such as DNA and protein fragments, in a single system[9–11]. Out of the available platforms, microarray-based microfluidic bioassay devices are rising to the forefront, owing to the ability to achieve multiple biomarker detection within a single system. This is largely attributed to the fact that multiple recognition biomolecules can be immobilized in well-defined micro- and nanoarrays on microfluidic device substrates, thereby allowing high precision screening of various biomarkers within a single device[12]. Although these systems have several significant advantages, there are several challenges that impede their routine usage in clinical diagnostics. First, it has proven to be a major challenge to integrate these micro/nanopatterned substrates within microfluidic devices, without significantly affecting the functionalities of the immobilized recognition biomolecules. Additionally, as the flow within the microfluidic channels generate high shear stresses, the immobilized biomolecules gradually desorb from the surfaces with time. This in turn proves to be a major drawback, as the reproducibility of these systems decreases as a result of the inconsistencies in

[a] Micro/Bio/Nanofluidics Unit, Okinawa Institute of Science and Technology Graduate University 1919-1 Tancha, Onna-son, Kunigami-gun Okinawa, Japan 904-0495
† Electronic Supplementary Information (ESI) available: [details of any supplementary information available should be included here]. See DOI: 10.1039/b000000x/
‡ These authors contributed equally to this work
* amy.shen@oist.jp

View Article Online
DOI: 10.1039/C7AN00273D

the number of available recognition biomolecules in the devices, throughout the course of the assay. Consequently, it is necessary to explore new technologies to overcome current limitations of biomolecule micro- and nanoarray fabrication within microfluidic devices.

Existing techniques to pattern biomolecules on surfaces in micro-[13] and nanoarrays, include physical patterning approaches such as photolithography[14], adsorption of biomolecules confined to microfluidic networks[15], and colloidal lithography[16]. These techniques are either plagued by high costs, low throughput, or limited control over the geometry and functional properties of the achieved patterns. Particularly, creating nanoarrays of biomolecules has been laborious and integration of these patterned substrates into microfluidic devices has been a challenge. A recent report proposed a self-assembly-based colloidal lithography technique to generate nanopatterns which were then sealed into PDMS microchannels to immobilize proteins onto the nanoarrays via non-covalent coupling[17]. Although the proposed method enables the successful generation of multiple protein nanoarrays within a microfluidic channel, the major drawbacks are the requirement of complex fabrication techniques to create the nanopatterned substrates, the repeated fabrication of new surfaces prior to each use, and the non-covalent coupling of proteins onto the nanoarrays inducing potential desorption when subjected to flow.

One of the simpler and preferred methods of patterning micro- and nanoscale features is microcontact printing ($\mu$CP), where chemical or biological molecules are transferred in designated patterns from an elastomeric poly(dimethylsiloxane) (PDMS) stamp onto a substrate with higher surface energy[18–21]. Although these microcontact printed biomolecules have been successfully incorporated into microfluidic devices[22,23], several challenges remain. First, as patterned biomolecules are physically adsorbed onto the surfaces driven by hydrogen-bonding and van der Waals forces[24], they are unable to withstand high shear stresses introduced by the flow present in microfluidic channels. As a result, it gives rise to gradual desorption and degradation of patterned biomolecules that lead to reduced device performance and poor shelf life. Secondly, since partial dehydration of biomolecules is a prerequisite to the $\mu$CP technique, the probability of protein denaturation and impaired biological activity is high. Additionally, the lack of control over the orientation of the printed proteins has been lamented and could be responsible for the suboptimal interactions in bioassays due to the inaccessibility of the binding sites. Lastly, patterning a substrate with multiple biomolecules proves to be difficult and time-consuming, as each individual stamp can only be utilized to pattern a single ink at a time.

To address these challenges, pre-patterned substrates have been used to covalently link the biomolecules from solution to pattern sensitive biomolecules. For example, Teerapanich *et al.* recently achieved real-time monitoring of protein-binding kinetics by creating patterned gold films to stably and covalently immobilize antibodies within nanofluidic channels[25]. Others have reported a simpler and more stable surface patterning technique that employs covalent coupling of proteins and nucleotides to silane treated substrates[26,27]. Recently, Lin *et al.* demonstrated a novel method of covalently patterning multiple proteins to a (3-glycidyloxypropyl)trimethoxysilane modified substrate enclosed within nanochannels by using a robotic microarray spotter[28]. However, alignment of the channels with the patterns is difficult to achieve since the proteins are deposited onto the substrates prior to the bonding of the device. Additionally, as the proteins are dried briefly before alignment, viability for long-term studies is a concern due to their potential degradation.

Alternatively, (3-aminopropyl)triethoxysilane (APTES), an amine–$NH_2$ terminated silane can be used to form covalent siloxane bonds with silica substrates under pertinent conditions[29]. Anhydrous organic solvents like toluene have been widely used to achieve homogeneity of the formed monolayers and to ensure covalent binding of APTES with the glass substrates[30]. These terminal amine groups then serve to covalently couple biomolecules with the help of appropriate linkers[31,32]. Several studies have demonstrated the potential of $\mu$CP to create patterns of APTES monolayers within microfluidic channels that are then covalently coupled with biomolecules from solution[33,34]. Although this method provides simplicity and potential for achieving multiplexing in microfluidic devices, the resolution of obtained features is not only limited by the microfluidic channel dimensions, but also by the printing process since existing $\mu$CP methods rely on the use of organic solvents that can potentially swell the PDMS substrate and increase the dimensions of the patterned features[35]. Although the degree of PDMS swelling does not significantly affect micron-size features in the stamps, it proves to be a limiting factor while attempting to achieve nanoarrays of APTES patterns. Notably, similar to thiols, silanes being small molecules, can diffuse into the PDMS stamp upon long incubation times[36]. As a result, during the printing step (on the order of minutes), silane molecules tend to diffuse out of the stamp along with the solvent molecules, reducing the resolution of the patterned features[37].

In this work, we present a new means of creating micro- and nanoarrays of aminosilanes within microfluidic devices via an aqueous based microcontact printing technique to subsequently create micro- and nanoarrays of biomolecules. To minimize the diffusion of APTES into the PDMS stamp during the printing process, we use water as the inking solvent and enforce short incubation and contact times to preserve the pre-defined resolution of patterned features[38]. These patterns then serve as the building block to couple multiple biomolecules in solution onto a single surface for subsequent multiplexed bioassays. We verify the multiplexing capability on a single patterned surface by delivering different biomolecules to different regions of the patterned array with the help of microfluidic networks and liquid dispensing technologies. Next, to validate the functionality of the coupled biomolecules, we carry out an aptamer-based immunoassay to detect interleukin 6 (IL6) and an antibody-based immunoassay for the detection of human c-reactive protein (hCRP). Finally, we probe the stability of APTES patterns and demonstrate the possibility of fabricating pre-stored and ready-to-use bioassay devices with a shelf life of at least 3 months.

View Article Online
DOI: 10.1039/C7AN00273D

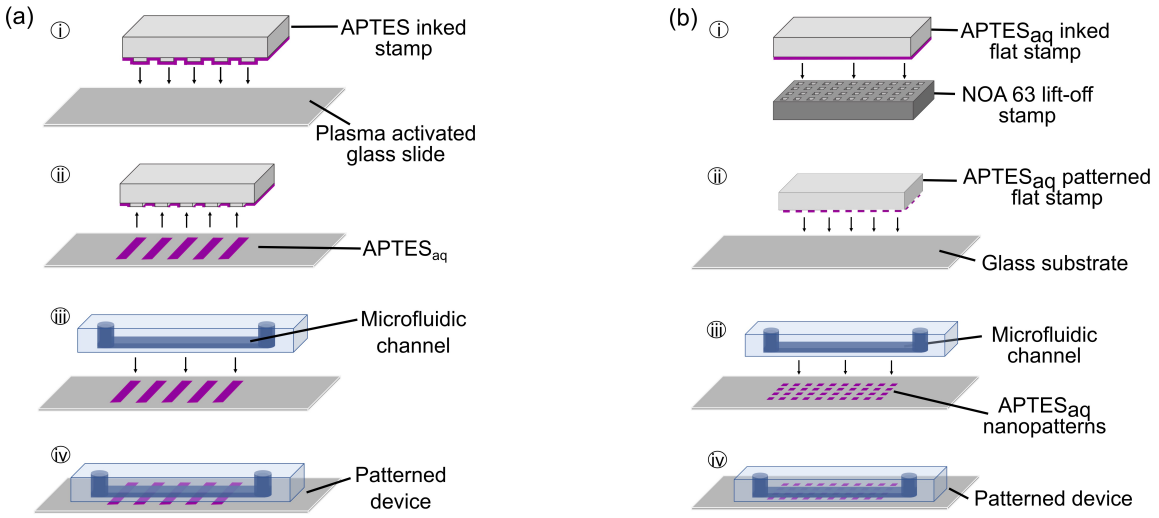


**Fig. 1 Fabrication of patterned microfluidic devices.** (a) Microcontact printing for $APTES_{aq}$ microarrays: (i) a PDMS stamp inked with $APTES_{aq}$ is contacted with a plasma activated glass surface through microcontact printing to (ii) transfer $APTES_{aq}$ microarrays (purple) onto the glass surface. (iii) A PDMS microfluidic channel is then bonded to the patterned glass substrate to create (iv) a sealed microfluidic device encapsulating $APTES_{aq}$ microarrays. (b) Lift-off nanocontact printing for $APTES_{aq}$ nanoarrays: (i) A plasma-activated NOA63 lift-off stamp was contacted with an $APTES_{aq}$–inked flat PDMS stamp. (ii) The $APTES_{aq}$ patterned flat stamp was pressed onto a plasma activated glass slide for 5 s. (iii) A microfluidic channel was then bonded irreversibly to (iv) encapsulate the nanoarrays.

## 2 Materials and methods

### 2.1 Reagents and materials

(3-Aminopropyl) triethoxysilane (APTES), 2-methoxy (polyethyleneoxy) 6-9 propyl tricholoro silane (PEG-silane) and Tween 20 were purchased from Nacalai Tesque, Inc., Japan. 1-ethyl-3-(3- dimethylaminopropyl) carbodiimide (EDC), N-hydroxysuccinimide (NHS), BS3 crosslinker, phosphate buffered saline (PBS), HEPES, glycine and streptavidin DyLight$^{TM}$550 Conjugated, were purchased from Thermo Fischer Scientific, Japan. Biotin-SP-conjugated AffiniPure goat anti-mouse antibody was purchased from Jackson ImmunoResearch labs, USA. Biotinylated aptamers specific to interleukin 6 (IL6) were obtained from BasePair Biotechnologies, USA. Recombinant human IL6 (PHC0066) was purchased from Life Technologies. Mouse anti-c reactive protein antibody [C5] ab8279 (Abcam, Japan) and recombinant human c-reactive protein (hCRP) were obtained from Oriental Yest Co., Ltd., Japan. Alexa Fluor 488 conjugated chicken anti-goat, Alexa Fluor 546 conjugated rabbit anti-mouse and goat anti-chicken immunoglobulins (IgGs) were purchased from Abcam, Japan.

### 2.2 Patterning and fabrication procedures

#### 2.2.1 Soft lithograhy

Stamps and microfluidic devices were designed with AutoCAD (AutoDesk, USA). Stamp designs comprised of (i) 100 $\mu$m wide stripes with 100 $\mu$m spacing (schematic in Figure 1a(i)), and (ii) an array of 50 by 50 $\mu$m squares (Figure 4a-b) separated by 50 $\mu$m. Three different designs of microfluidic devices were designed in AutoCAD: (i) 100 $\mu$m wide and (ii) 200 $\mu$m wide parallel channels with single inlet, for unidirectional flow; and (iii) 200 $\mu$m wide parallel channels with two different inlets, for opposite flow directions in alternating channels. More detailed schematics are illustrated in Figure S1 in the SI document. For fabricating the master for the devices and stamps, silicon wafers (4-inch in diameter, E&M Corp. Ltd., Japan) were coated with a 75 $\mu$m layer of mr-DWL 40 photoresist (Microresist technologies, Germany), and the features were patterned by photolithography using a DL1000 maskless writer (NanoSystem Solutions, Japan) and developed by using mr-Dev 600 developer (Microresist Technologies, Germany). After thorough baking and cleaning, the wafers were coated with an antiadhesive layer by exposing it to trichloro(1H, 1H, 2H 2H-perfluorooctyl) silane (Sigma-Aldrich, Japan) in vapor phase in a desiccator. Microfluidic devices and stamps with the inverse copy of the pattern present on the Si-wafer were obtained by pouring 10:1 poly-(dimethylsiloxane) (PDMS) (DOW Corning, Japan) on the wafer and curing the pre-polymer for 24 h at 60 °C after degassing to remove air bubbles. For the lift-off nanocontact printing process, flat PDMS stamps were fabricated by polymerizing the afore mentioned mixture on a blank Si-wafer.

#### 2.2.2 Microcontact printing ($\mu$CP) in microfluidic devices

As illustrated in the schematic in Figure 1a, the micropatterned stamps were inked with 10 $\mu$L of 1% aqueous APTES ($APTES_{aq}$) by volume for 1-3 min under a plasma activated coverslip. The stamps were rinsed with milli-Q water (Millipore, Japan) for 10 s before rapid drying with a strong pulse of $N_2$ gas. The inked PDMS stamp was then contacted with a plasma activated (Harrick Plasma, USA) glass slide for 5 s (Figure 1a(i)-(ii)). The prepared plasma-activated PDMS microfluidic channel mould was bonded, perpendicular to the printed substrate to create the microarrays (Figure 1a(iii)-(iv)). The assembled device was then heated at 85°C for 5 minutes on a hot plate to simultaneously (a) drive the formation of a covalent siloxane bond between the reactive

View Article Online
DOI: 10.1039/C7AN00273D

silanols and the hydroxyl (-OH) groups on the glass substrate[39], and (b) to irreversibly bond the microfluidic device to the substrate.

#### 2.2.3 Nanopatterned lift-off stamps

Nanopatterned PDMS replicas were fabricated using the protocol previously described by Ricoult, et al.[40]. Briefly, nanopatterns consisting of a square array (200 nm in length, 200 nm in width, with 2 $\mu$m in spacing) were first created using Clewin Pro 4.0 (Wieweb software, Hengelo, Netherlands). A 4-inch silicon wafer was coated with PMMA resist and the dot arrays were patterned by electron beam lithography (VB6 UHR EWF, Vistec), followed by 100 nm reactive ion etching (System100 ICP380, Plasmalab) into the Si. After cleaning, the wafer was coated with an anti-adhesive layer by exposing it to perfluorooctyltriethoxysilane (Sigma-Aldrich, Oakville, ON, Canada) in vapor phase in a desiccator. An inverse polymer copy of the Si wafer was obtained after curing PDMS on the patterned wafer as described in the previous section to generate nanopillars. The lift-off stamp consisting of nanoholes with an inverse copy of the PDMS master (Figure 3a) was finally obtained by curing Norland Optical Adhesive 63 (NOA63, Norland Products, Cranbury, NJ) on the PDMS stamp with 600 W of UV light for 40 seconds in a Uvitron 600W UVA Enhanced Lamp (310-400 nm; 100% intensity) (Uvitron International, Inc., West Springfield, MA). NOA63 is an optically sensitive adhesive that polymerises on exposure to ultraviolet(UV) light.

#### 2.2.4 Lift-off nanocontact printing

A flat PDMS stamp was inked for 1-3 min with the 1% $APTES_{aq}$ solution as mentioned above (Figure 1b). After rinsing with milli-Q water for 10 s, the inked stamps were briefly dried under a stream of $N_2$ and immediately brought into contact with a plasma activated NOA63 lift-off stamp for 5 s (Figure 1b(i)). The PDMS was separated from the NOA63 lift-off stamp and the $APTES_{aq}$ in the contact area were transferred to the NOA63 lift-off stamp, while the remaining $APTES_{aq}$ molecules were transferred to the final substrate by printing the PDMS stamp for 5 s onto a plasma activated glass surface (Figure 1b(ii)). As described in Section 2.2.2, the plasma-activated PDMS microfluidic channel is finally bonded to the glass substrate to encapsulate the nanoarrays (Figure 1b(iii)-(iv)) and heated at 85°C for 5 minutes on a hot plate (Figure 1b(iii)-(iv)).

### 2.3 $APTES_{aq}$–biomolecule grafting within patterned devices

Following $APTES_{aq}$ patterning and device assembly, the unpatterned regions within the device were blocked for 30 min by flowing a solution of 2 wt% $PEG\text{-}silane_{aq}$ through the device. Flow rates of 2 $\mu$L/min were used to pump fluids through the channels for all experiments described below. Additionally, the unreacted molecules were washed out of the channels by flowing a wash buffer that consisted of 1×PBS (phosphate buffer saline) mixed with 0.05% Tween 20[41], for 10 minutes after every step of the reaction in all the experiments. Fluorescently labelled immunoglobulins or protein of interest at 10 $\mu$g/ml were flowed through the channels for 30 minutes to covalently graft the proteins on the $APTES_{aq}$ patterned surface by employing EDC-NHS chemistry at a 10–fold molar excess of EDC (2 $\mu$M) and NHS (5 $\mu$M) to protein (see Figure 2a & b). Similarly, DNA aptamers were grafted using BS3 (bis(sulfosuccinimidyl)suberate) chemistry where 100 $\mu$M of BS3 in milli-Q water was flowed over the patterns for 30 mins in the device to enable reaction with the available terminal amine ($-NH_2$) group on the $APTES_{aq}$, followed by the aptamer solution (10 $\mu$g/ml) in 20 mM HEPES buffer for 30 mins and 50 mM of $Glycine_{aq}$ to quench unreacted BS3 for an additional 30 mins. Unreacted components were washed with wash buffer (0.05% Tween 20 in 1× PBS) following each step of the reaction.

### 2.4 Immunoassay

For the aptamer-based immunoassay, 10 $\mu$g/ml of $-NH_2$-terminated aptamers specific to interleukin 6 (IL6) were grafted onto the $APTES_{aq}$ microarrays via BS3 chemistry after blocking (Section 2.3). Flow rates of 2 $\mu$L/min were used to deliver the solutions through the channels for all steps of the experiments described below. Subsequently, 470 nM of IL6 was flowed through the channels for 30 mins and detected with the help of a complimentary biotinylated detection aptamer (10 $\mu$g/ml) and streptavidin dye that were flowed through the same channels for 30 mins each. To carry out an antibody-based sandwich immunoassay to detect c-reactive protein (hCRP), capture antibodies against hCRP were grafted onto $APTES_{aq}$ microarrays via BS3 chemistry (Section 2.3). Varying concentrations from 2 nM to 217 nM of hCRP mixed in 1×PBS were flowed through microchannels of different devices patterned with capture antibodies against hCRP for 30 mins respectively. The reaction was detected by a detection antibody pair that consisted of the same capture antibodies and complimentary Alexa-fluor 546-labelled fluorescent secondary antibodies (10 $\mu$g/ml), see detailed schematic in Figure 5b. Given the pentameric structure of hCRP, the same capture antibody was used as the detection antibody at a concentration of 10 $\mu$g/ml, flowed for 30 mins through the microchannels. Unreacted components were washed with wash buffer (0.05% Tween 20 in 1× PBS) for 10 mins, following each step of the reaction. The flow rates and incubation times used in this work were selected to demonstrate proof-of-concept immunoassay reactions, and can be further optimized as per immunoassay requirements.

### 2.5 Imaging and analysis

NOA63 lift-off stamps were imaged using Quanta 250 FEG scanning electron microscope (FEI, Japan) at 5 kV with a spot size of 3.5 using an ETD Detector to detect secondary electrons. Micro- and nanopatterns of fluorescently labeled protein were imaged on a Ti-E Eclipse inverted fluorescent microscope (Nikon, Japan) and an LSM 780 Confocal microscope (Zeiss, Japan). All images were captured with fixed exposure times within each experiment, which varied from 1 to 10 s for all the images shown in this work. Mean fluorescence intensity measurements were obtained by performing image analysis in ImageJ (NIH, USA). Images were processed post quantification to increase the contrast through linear modifications in ImageJ.

View Article Online
DOI: 10.1039/C7AN00273D

## 3 Results and discussions

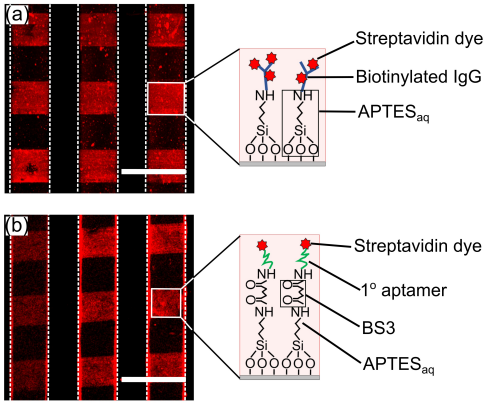


**Fig. 2 Microarrays of IgGs and DNA aptamers in APTES$_{aq}$ patterned microfluidic devices.** (a) Biotinylated IgGs were grafted on the APTES$_{aq}$ patterns via EDC-NHS chemistry and labeled with fluorescent streptavidin dye (in red) to reveal an array of 100 $\mu$m squares within the microfluidic channels. (b) Alternatively, amine-terminated biotinylated primary aptamers (1° aptamer) were immobilized to the APTES$_{aq}$ microarray via BS3 chemistry and subsequently stained with streptavidin dye. Dotted lines depict microfluidic channel boundaries and scale bars are 200 $\mu$m. Illustrations portray the binding architecture of molecules within the patterns.

### 3.1 APTES$_{aq}$ microarrays for grafting of biomolecules within microfluidic devices

A microcontact printing process was developed to print microarrays of aqueous APTES (APTES$_{aq}$) in closed microfluidic devices. These APTES micropatterns then serve to covalently couple various types of biomolecules to subsequently create the biomolecule microarrays within the microfluidic devices. As described in Section 2.3, APTES$_{aq}$ was printed in microarray geometries, enclosed within the horizontal microfluidic channels (schematic in Figure 1a) and covalently coupled with the desired biomolecules. Here, 2% PEG-silane$_{aq}$ was used to block non-specific sites since it not only acts as a non-biofouling agent but also prevents diffusion of APTES$_{aq}$ on the patterned substrate.

Figure 2a & b depict grafting of biotinylated immunoglobulins (IgGs) via EDC–NHS chemistry and amine (–$NH_2$)-terminated biotinylated aptamers using BS3 (bis(sulfosuccinimidyl)suberate), an –$NH_2$ to –$NH_2$ linker, onto APTES patterns respectively. These patterned biotinylated molecules were then subsequently labeled with fluorescent streptavidin dye to reveal their successful covalent grafting as red squares within the microfluidic channels. Additionally, the integrity of the biomolecule patterns under high shear stresses in the microfluidic channels was confirmed as shown in Supplementary Figure S2.

In previously described methods[34], when the silanes were inked with toluene, there is a high probability of PDMS swelling and subsequent change in feature sizes. Additionally, silane-toluene reservoirs are created within the stamp, which diffuse out of the stamp when printed onto glass surfaces for long contact times,[37] ultimately leading to loss of resolution. With our protocol, by using water as the inking solvent, we not only limit the probability of silane reservoir formation and swelling of the stamp, but also reduce leakage upon contact by using combined inking and printing times on the order of a few minutes. Thus, the desired patterning dimension is maintained during and after the printing process, a prerequisite for high-efficiency microarray applications. These results depict the compatibility of this technique with glass-based microfluidic devices to create microarrays of not only proteins but also effectively couple other biomolecules such as DNA aptamers covalently onto their substrates for subsequent bioassay applications.

### 3.2 Aminosilane nanoarrays for biomolecule immobilization within microfluidic devices

In addition to successfully creating microarrays of APTES to covalently pattern biomolecules, we further demonstrate a simple lift-off nanocontact printing method for creating nanoarrays of APTES$_{aq}$ within microfluidic channels to subsequently graft biomolecules covalently. Generally, PDMS stamps with pillars of desired shapes are employed for the microcontact printing process. These pillars are of microscale dimensions and are less susceptible to collapse when pressed onto a substrate. Therefore, the patterned features are intact after transfer. However, if the dimensions of the pillars are reduced down to the nanoscale, the pillars are highly susceptible to collapse when pressed onto the substrate. This in turn leads to loss of resolution of desired nanoscale features[42]. Hence, to pattern high resolution arrays with nanometer scale geometries, the use of patterned stamps with nanopillars was avoided. Alternatively, a two-stamp process utilizing NOA63 lift-off stamps (Figure 3a) and PDMS flat stamps, was employed to pattern nanoarrays of APTES$_{aq}$ on glass substrates of microfluidic devices. Here, the final pattern is printed using a flat PDMS stamp to avoid loss of resolution (Sec-

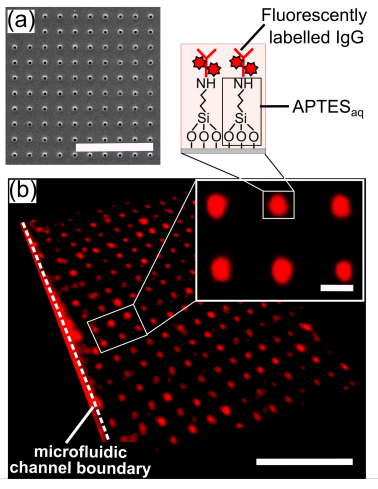


**Fig. 3 Lift-off nanocontact printing for APTES nanoarrays.** (a) SEM image depicting the nanoholes on the surface of an NOA63 lift-off stamp. (b) Confocal microscopy image of fluorescently-labeled IgGs grafted onto the APTES$_{aq}$ nanoarrays within the microfluidic channels. The illustration depicts the binding architecture within patterns. Scale bars in (a) & (b) are 5 $\mu$m and 500 nm in the inset of (b).

View Article Online
DOI: 10.1039/C7AN00273D

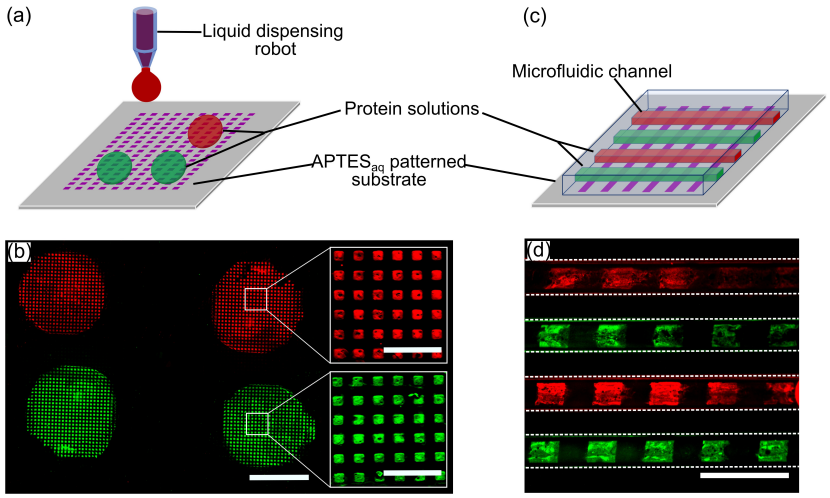


**Fig. 4 Multiplexed protein microarrays on APTES$_{aq}$ micropatterns using liquid dispensing robots and microfluidic devices.** (a) Schematic illustrating a liquid dispensing robot delivering two different protein solutions to different portions of an APTES$_{aq}$ patterned substrate. (b) A liquid dispensing robot was used to locally deliver EDC–NHS activated Alexa-fluor 488 (green) and 546-labelled fluorescent antibodies (red) to different regions of an APTES$_{aq}$ array blocked with PEG-silane$_{aq}$. (c) Microcontact printing of an array of 100 $\mu$m wide APTES$_{aq}$ stripes was carried out prior to bonding of a microfluidic device containing channel arrays that were aligned perpendicular to each other. (d) Blocking was carried out using PEG-silane$_{aq}$ prior to delivering solutions of fluorescently-labeled IgGs to alternating channels. After washing, a microarray of alternating patterns of red and green-labeled IgG are created within the microfluidic channels. Scale bars are 2 mm in (b), 300 $\mu$m in the insets of (b), and 300 $\mu$m in (d).

tion 2.2.4). Subsequently, fluorescently-labeled IgGs were grafted onto the APTES$_{aq}$ nanopatterns via EDC-NHS chemistry to reveal 200 nm nanoarrays of proteins within the microfluidic channels (Figure 3b).

Several prior studies have reported the potential of nanocontact printing for the creation of biomolecule nanoarrays. However, few reports have incorporated these patterns into microfluidic devices for subsequent microfluidic bioassays[17]. Additionally, the reliance of the nanocontact printing process on physisorption proves to be a drawback, as the biomolecules are susceptible to detachment from the surface due to the presence of high shear stress introduced by the flow. Our new protocol here addresses all these challenges: by employing lift-off nanocontact printing of APTES$_{aq}$ on glass substrates, covalently tethered nanopatterns of proteins with a resolution of 200 nm can be easily integrated into microfluidic devices. Additionally, these protein nanopatterns are created with the same efficiency as the previously described direct nanocontact printing approach by Ricoult, et al.[40], see more details in Figure S3 of the SI document. Although DNA nanoarrays have been used over the years for various applications in the field of genomics for high-throughput DNA screening[43,44], there are fewer technologies that utilize protein nanoarrays in microfluidic platforms for disease diagnostics. This is mainly attributed to the difficulties in creating robust protein nanoarrays[45] within microfluidic devices. Addressing this major challenge, our newly developed technique can create robust, cheap and simple multiplexed microfluidic nanoarrays that will enable high-throughput protein and DNA detection with high reproducibility and ease.

### 3.3 Multiplexing on aminosilane microarrays

Although microcontact printing has been widely used for the creation of biomolecule microarrays[46], it has proven to be a daunting task to pattern multiple biomolecules on a single substrate with this technique. To overcome the one stamp–one ink characteristic of microcontact printing, we use APTES$_{aq}$ microarrays to capture and covalently graft different locally delivered biomolecules. To visually demonstrate the capability of patterning multiple biomolecules onto a single surface, two different solutions of EDC–NHS activated Alexa-fluor 488 (green) and 546-labelled fluorescent antibodies (red) were delivered onto the patterned substrate by two modes of liquid delivery. First, an array of squares (50 by 50 $\mu$m) of APTES$_{aq}$ was patterned on a plasma activated glass slide by microcontact printing and blocked with 2% PEG-silane$_{aq}$. Liquid dispensing robots (Musashi Engineering, Japan) were then used to deliver microliter volumes of droplets containing the two protein solutions (Figure 4a) to achieve a microarray composed of multiple biomolecules on the patterned surface (Figure 4b).

Alternatively, microfluidic devices (Figure 4c) with channel arrays were bonded on an array of 100 $\mu$m wide APTES$_{aq}$ stripes aligned perpendicular to the direction of the microfluidic channels. After blocking with PEG-silane$_{aq}$, the two solutions of EDC-NHS activated fluorescently-labeled antibodies (red and green) were fed into the channels and covalently grafted onto the APTES$_{aq}$ patterns within the channels (Figure 4d).

One of the major obstacles in achieving multipatterning by microcontact printing has been the necessity of fabrication of complex stamps that either contained microfluidic circuits or gradient generators on the stamp to create patterned concentration gradients on substrates. In comparison, the aminosilane printing approach coupled with microfluidics introduced in this work, facilitates the creation of large and stable arrays composed of multiple biomolecules presented via covalent bonds in a single device. By making use of the localized delivery available in microfluidic devices or liquid dispensing platforms, multi-protein patterns could

View Article Online
DOI: 10.1039/C7AN00273D

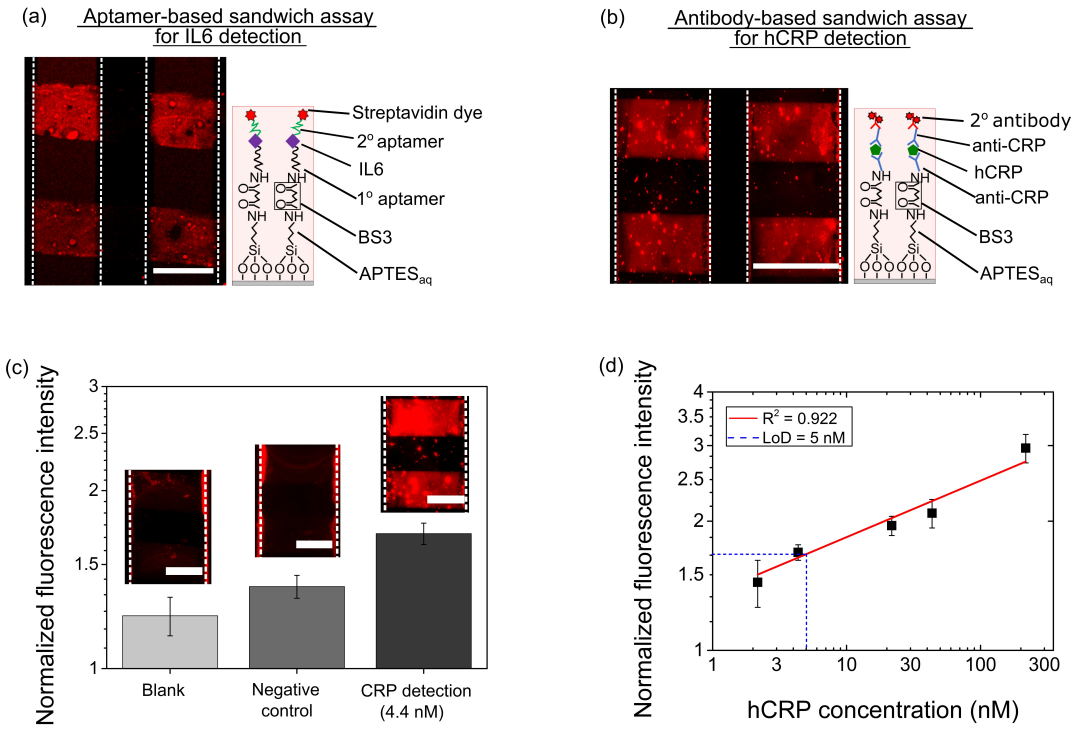


**Fig. 5 Aptamer and antibody-based immunoassay in APTES$_{aq}$ patterned devices.** (a) Aptamer-based sandwich immunoassays (via primary capture aptamers (1° aptamer) and secondary detection aptamers (2° aptamer)), and (b) antibody-based immunoassays (via primary capture antibodies (anti-CRP) and secondary detection antibody pairs (anti-CRP and 2° antibody)) were carried out to detect of IL6 and hCRP on aptamer-functionalized and antibody-functionalized APTES$_{aq}$ microarrays respectively in microfluidic devices. (c) Histogram of normalized fluorescence intensity values is plotted for detection of 4 nM of hCRP versus that of blank and negative control (IL6). (d) Normalized fluorescence intensity values are plotted for the tested concentrations of hCRP. The red solid line depicts the best curve fit and the dotted blue lines depict the limit of detection where the lowest concentration of hCRP detected was 4 nM. Scale bars are 100 $\mu$m for (a) & (c) and 200 $\mu$m for (b).

easily be achieved within a single array. Additionally, with the advent of nanofluidic devices[47] and liquid dispensing robots delivering picolitre droplets, densely packed nanoarrays can undoubtedly be achieved in the near future.

### 3.4 Aptamer-based and antibody-based immunoassays

To test the sensitivity and validate biofunctionality of our APTES$_{aq}$-micropatterned microfluidic devices, sandwich-based immunoassays were carried out to detect interleukin 6 (IL6) and human c-reactive protein (hCRP) with the help of either aptamers or antibodies respectively. IL6[48,49] and hCRP[50,51] are the most important biomarkers of neurological, cardiovascular and other pathophysiological conditions that arise from tissue inflammation or infection. Quantitative detection of these biomarkers has immensely helped in early diagnosis and treatment of these diseases. In order to accurately diagnose these diseases, sensitive assays and biosensing technologies are required to reliably detect minute quantities of these biomarkers[52–54]. Therefore, to test the functionalities of our microarray microfluidic devices, aptamer and antibody-based immunoassays were performed to qualitatively and quantitatively detect IL6 and hCRP.

Aptamer-based immunoassays were carried out using the protocol described in Section 2.4 to succesfully detect 470 nM of IL6 (Figure 5a). Next, to detect hCRP, an antibody-based sandwich immunoassay was carried out on APTES$_{aq}$ microarrays in microfluidic devices (Figure 5b). To further characterize the sensitivity of these patterned devices, we focused on the antibody-based sandwich immunoassay. A range of concentrations of hCRP from 4–200 nM was successfully detected via the detection antibody pair and qualitatively analyzed by fluorescence microscopy (more details are shown in Figure S4a-e in the SI document).

To estimate the detection of hCRP quantitatively, the normalized fluorescence intensity was calculated for each condition by measuring the ratio of mean pixel intensity of the patterned region (red) to that of the unpatterned region (black), averaged over 3 images each with 9 patterned squares in each image. A blank reaction was carried out by flowing the detection antibody pair over the grafted capture antibody to account for the non-specific adsorption. The histogram in Figure 5c depicts the normalized fluorescence intensity plotted for positive detection of the lowest detectable concentration of 4.4 nM of hCRP versus that of the blank reaction and a negative control (i.e., IL6 flowed through the anti-hCRP grafted microchannels). Since the same primary antibody was used as both the capture and detection antibodies, it is likely to be responsible for the non-specific adsorption observed in these devices.

Figure 5d displays the normalized fluorescence intensity values captured for each concentration of hCRP detected (in black

View Article Online
DOI: 10.1039/C7AN00273D

squares), while the solid red line is the best linear curve fit[55] with an $R^2$ value of 0.922. Results illustrate that the lowest detectable concentration of hCRP in these patterned devices was 4 nM as estimated by the limit of detection calculated to be 1.67 relative fluorescence units (RFU), derived from the following formula[56]:

$$LoB = Mean_{blank} + 1.645(SD_{blank}), \quad (1)$$

$$LoD = LoB + 1.645(SD_{lcs}) \quad (2)$$

where *LoB*, *SD*, *LoD* and *lcs* are the limit of blank, standard of deviation, limit of detection and lowest concentration sample respectively.

The successful detection of clinically significant levels of IL6 and hCRP validates the biofunctionality of these patterned devices. The sensitivity of these devices can be significantly improved in the future with more specific aptamer or antibody combinations coupled with label-free detection systems.

### 3.5 Stability of aminosilane microarrays

To assess the stability of the $APTES_{aq}$ microarrays, microfluidic device substrates were pre-patterned with $APTES_{aq}$ by microcontact printing perpendicular to the microfluidic channels, in stripes of 100 $\mu$m separated by 100 $\mu$m in spacing. Thirty patterned and sealed devices were stored in plastic containers after blocking with PEG-$silane_{aq}$ for up to 3 months at room temperature (25°C) or at 4°C in the absence of vacuum. Three devices per testing condition were characterized to determine the efficiency of grafting of fluorescently labeled IgGs (immunoglobulins) on the $APTES_{aq}$ microarrays.

Square fluorescent bands shown in Figure 6a-f illustrate successful grafting of the IgGs. To quantify the efficiency of grafting, fluorescent squares were considered as signal and unpatterned regions as background. Normalized fluorescence intensity values were quantified by ImageJ using the same method of analysis as previously described, and plotted for each of the testing conditions (3 devices per condition) (Figure 6g), where the standard deviations indicate averaging uncertainty. Figure 6 demonstrates that the $APTES_{aq}$ is stable for 3 months when stored at either 4°C or 25°C and can be used to graft biomolecules prior to immunoassay to eliminate the concern of biodegradation arising from the storage of patterned biomolecules.

It is worth noting that the initially microcontact printed $APTES_{aq}$ patterns already have a small level of inhomogeneity as seen in Figure 6a & d. This may be due to the oligomerization of highly reactive $APTES_{aq}$ molecules in water that form aggregates when inked on the stamp before the printing process[57,58]. This can be reduced by preparing fresh aqueous $APTES_{aq}$ solution prior to the inking process, reducing inking times and eliminating the step where the inked stamp is rinsed with water prior to print. Although the presence of fluorescently-labelled IgGs on devices stored for 3 months depicts presence of $APTES_{aq}$ (Figure 6g), gradual degradation of $APTES_{aq}$ is seen with time (Figure 6c & f). As elucidated in previous literature[59] this degradation could be either owing to (i) moisture aided decomposition of $APTES_{aq}$[60] due to the high humidity environment present while performing

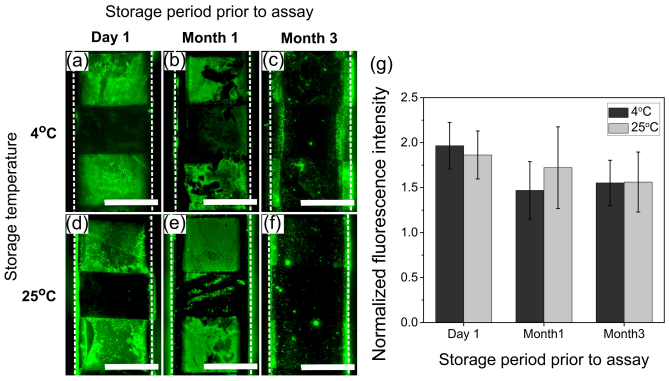


**Fig. 6 $APTES_{aq}$ microarrays in microfluidic devices are stable for 90 days at both 4°C and room temperature.** Fluorescently labeled IgGs (green) were grafted on Day 1, Month 1 and Month 3 onto 6 different $APTES_{aq}$–patterned microfluidic devices stored at 4°C ((a), (b) & (c)) and at 25°C ((d), (e) & (f)) respectively. (g) The histogram depicts the normalized fluorescence intensity, quantified on the $APTES_{aq}$ patterns for three tested conditions. Scale bars are 100 $\mu$m.

the experiments, (ii) gradual self $-NH_2$-catalyzed hydrolysis and removal of the covalent siloxane of $APTES_{aq}$[39], or (iii) incomplete covalent binding of $APTES_{aq}$ to the glass substrate[30]. Additionally, an increase in normalized fluorescence intensities was observed for the devices grafted on month 1 versus month 3 when stored at 4°C. This is potentially caused by the presence of large number of IgG aggregates in the devices grafted on month 3 as seen in Figure 6c. These aggregates contribute significantly to the average fluorescence signals, thereby leading to an increase in the normalized intensity.

By printing aminosilane microarrays that are insensitive to enzymes and subsequently capturing the biomolecules at the time of the bioassay, we highlight the following advantages: 1) the patterned substrates can be stored on the order of months before carrying out the bioassay, 2) biomolecules are less likely to be affected by denaturation associated with external stresses since they are delivered in solution, and 3) interaction sites can be accurately engineered by precisely designing the silanes and biomolecules thereby providing control over the orientation of the biomolecules. Additional experiments are being carried out to further probe and improve the homogeneity and chemical viability of $APTES_{aq}$ microarrays on substrates upon storage, which will be reported in the future.

## 4 Conclusions

To create biomolecular micro- and nanoarrays within microfluidic channels, we introduced a micro- and nanocontact printing method to pattern amino terminated silanes on a desired planar surface, with feature sizes ranging from a few hundred microns down to 200 nm. This protocol provides several key advantages. First, owing to its compatibility with PDMS, water can be used as the inking solvent to pattern APTES arrays onto glass substrates. Next, the microfluidic channels deliver a blocking solution, to (i) limit the diffusion of volatile silanes as well as (ii) inhibit biofouling. APTES micro- and nanoarrays can be grafted with different biomolecules such as proteins and DNA in controlled orientations

View Article Online
DOI: 10.1039/C7AN00273D

for subsequent immunoassay applications within these devices. Additionally, the $APTES_{aq}$ microarrays maintain their ability to covalently graft biomolecules to the surface for at least 3 months after printing with no significant difference between storage conditions at room temperature or at 4°C, thereby demonstrating their storage potentials. By grafting biomolecules onto pre-patterned substrates prior to use, it greatly preserves the functionalities of the grafted biomolecules with minimized risks of biodegradation, accompanied by simplified operation protocols.

To demonstrate the multiplexing potentials of this technology, localized delivery available in microfluidic devices or liquid dispensing platforms were used to achieve multi-protein patterning within a single array. By exhibiting successful DNA-based immunoassays and antibody-based immunoassays carried out on microcontact printed aminosilane microarrays, we validated the biofunctionality of these devices thereby elucidating the overall potential of this technology in the field of bioassay applications.

Applications for biomolecule micro- and nanoarrays are broad[43,61,62], but their translation from the lab to commercial products has been hindered by limited abilities to integrate micro- and nanoscale patterns into microfluidic devices with high precision. With our simple patterning technique, robust micro- and nanoarrays of different biomolecules can be created with ease within microfluidic devices for next-generation high-throughput biomarker detection.

## 5 Acknowledgements

The authors thank Professor David Juncker and Professor Tohid Didar for valuable discussions while djlab provided valuable materials. We also wish to thank Kieran Deasy, Laszlo Szikszai, Mandy Leung, Nikhil Bhalla, Casey Galvin and Abhishek Sinha for technical support and discussions. We acknowledge financial support from the OIST Graduate University with subsidy funding from the Cabinet Office, Government of Japan.

## References

1 W. Su, X. Gao, L. Jiang and J. Qin, *Journal of Chromatography A*, 2015, **1377**, 13–26.
2 D. G. Rackus, M. H. Shamsi and A. R. Wheeler, *Chemical Society Reviews*, 2015, **44**, 5320–5340.
3 M. Karle, S. K. Vashist, R. Zengerle and F. von Stetten, *Analytica chimica acta*, 2016, **929**, 1–22.
4 V. C. Rucker, K. L. Havenstrite, B. A. Simmons, S. M. Sickafoose, A. E. Herr and R. Shediac, *Langmuir*, 2005, **21**, 7621–7625.
5 G. Du, Q. Fang and J. M. den Toonder, *Analytica chimica acta*, 2016, **903**, 36–50.
6 A. Karimi, D. Karig, A. Kumar and A. Ardekani, *Lab on a Chip*, 2015, **15**, 23–42.
7 N. D. Gallant, J. L. Charest, W. P. King and A. J. García, *Journal of nanoscience and nanotechnology*, 2007, **7**, 803–807.
8 S. Takayama, J. C. McDonald, E. Ostuni, M. N. Liang, P. J. Kenis, R. F. Ismagilov and G. M. Whitesides, *Proceedings of the National Academy of Sciences*, 1999, **96**, 5545–5548.
9 P. Angenendt, J. Glökler, Z. Konthur, H. Lehrach and D. J. Cahill, *Analytical chemistry*, 2003, **75**, 4368–4372.
10 S. Choi, M. Goryll, L. Y. M. Sin, P. K. Wong and J. Chae, *Microfluidics and Nanofluidics*, 2011, **10**, 231–247.
11 C. K. Tang, A. Vaze, M. Shen and J. F. Rusling, *ACS sensors*, 2016, **1**, 1036–1043.
12 C. K. Dixit and G. R. Aguirre, *Microarrays*, 2014, **3**, 180–202.
13 K. Jang, Y. Xu, K. Sato, Y. Tanaka, K. Mawatari and T. Kitamori, *Microchimica Acta*, 2012, **179**, 49–55.
14 E. E. Hui and S. N. Bhatia, *Langmuir*, 2007, **23**, 4103–4107.
15 J. L. Garcia-Cordero and S. J. Maerkl, *Chemical Communications*, 2013, **49**, 1264–1266.
16 M. A. Ray, N. Shewmon, S. Bhawalkar, L. Jia, Y. Yang and E. S. Daniels, *Langmuir*, 2009, **25**, 7265–7270.
17 A. S. Andersen, W. Zheng, D. S. Sutherland and X. Jiang, *Lab on a Chip*, 2015, **15**, 4524–4532.
18 M. Mrksich and G. M. Whitesides, *Trends in biotechnology*, 1995, **13**, 228–235.
19 L. Filipponi, P. Livingston, O. Kašpar, V. Tokárová and D. V. Nicolau, *Biomedical microdevices*, 2016, **18**, 1–7.
20 R. Castagna, A. Bertucci, E. A. Prasetyanto, M. Monticelli, D. V. Conca, M. Massetti, P. P. Sharma, F. Damin, M. Chiari, L. De Cola *et al.*, *Langmuir*, 2016, **32**, 3308–3313.
21 S. A. Lange, V. Benes, D. P. Kern, J. H. Hörber and A. Bernard, *Analytical chemistry*, 2004, **76**, 1641–1647.
22 R. S. Kane, S. Takayama, E. Ostuni, D. E. Ingber and G. M. Whitesides, *Biomaterials*, 1999, **20**, 2363–2376.
23 E. B. Chakra, B. Hannes, J. Vieillard, C. D. Mansfield, R. Mazurczyk, A. Bouchard, J. Potempa, S. Krawczyk and M. Cabrera, *Sensors and Actuators B: Chemical*, 2009, **140**, 278–286.
24 W. Norde, *Colloids and Surfaces B: Biointerfaces*, 2008, **61**, 1–9.
25 P. Teerapanich, M. Pugnière, C. Henriquet, Y.-L. Lin, C.-F. Chou and T. Leïchlé, *Biosensors and Bioelectronics*, 2017, **88**, 25–33.
26 Y. Wu, T. Buranda, R. L. Metzenberg, L. A. Sklar and G. P. Lopez, *Bioconjugate Chemistry*, 2006, **17**, 359–365.
27 H. H. Weetall, *Applied Biochemistry and Biotechnology*, 1993, **41**, 157–188.
28 Y.-L. Lin, Y.-J. Huang, P. Teerapanich, T. Leïchlé and C.-F. Chou, *Biomicrofluidics*, 2016, **10**, 034114.
29 N. Aissaoui, L. Bergaoui, J. Landoulsi, J.-F. Lambert and S. Boujday, *Langmuir*, 2011, **28**, 656–665.
30 R. M. Pasternack, A. S. Rivillon and Y. J. Chabal, *Langmuir*, 2008, **24**, 12963–12971.
31 S. K. Vashist, E. Lam, S. Hrapovic, K. B. Male and J. H. Luong, *Chemical reviews*, 2014, **114**, 11083–11130.
32 S. Kuddannaya, Y. J. Chuah, M. H. A. Lee, N. V. Menon, Y. Kang and Y. Zhang, *ACS applied materials & interfaces*, 2013, **5**, 9777–9784.
33 T. F. Didar, A. M. Foudeh and M. Tabrizian, *Analytical chemistry*, 2011, **84**, 1012–1018.
34 G. Arslan, M. Özmen, I. Hatay, I. H. Gübbük and M. Ersöz,

View Article Online
DOI: 10.1039/C7AN00273D

*Turkish Journal of Chemistry*, 2008, **32**, 313–321.
35 J. N. Lee, C. Park and G. M. Whitesides, *Analytical Chemistry*, 2003, **75**, 6544–6554.
36 T. E. Balmer, H. Schmid, R. Stutz, E. Delamarche, B. Michel, N. D. Spencer and H. Wolf, *Langmuir*, 2005, **21**, 622–632.
37 Y. Xia and G. M. Whitesides, *Annual review of materials science*, 1998, **28**, 153–184.
38 H. Li, J. Zhang, X. Zhou, G. Lu, Z. Yin, G. Li, T. Wu, F. Boey, S. S. Venkatraman and H. Zhang, *Langmuir*, 2009, **26**, 5603–5609.
39 J. A. Howarter and J. P. Youngblood, *Langmuir*, 2006, **22**, 11142–11147.
40 S. G. Ricoult, M. Pla-Roca, R. Safavieh, G. M. Lopez-Ayon, P. Grütter, T. E. Kennedy and D. Juncker, *Small*, 2013, **9**, 3308–3313.
41 L. DeForge and D. Remick, *Immunological investigations*, 1991, **20**, 89–97.
42 C. Hui, A. Jagota, Y. Lin and E. Kramer, *Langmuir*, 2002, **18**, 1394–1407.
43 R. Drmanac, A. B. Sparks, M. J. Callow, A. L. Halpern, N. L. Burns, B. G. Kermani, P. Carnevali, I. Nazarenko, G. B. Nilsen, G. Yeung *et al.*, *Science*, 2010, **327**, 78–81.
44 J. C. White, *PhD thesis*, University of Birmingham, 2016.
45 C. Mosher, M. Lynch, S. Nettikadan, W. Henderson, A. Kristmundsdottir, M. W. Clark and E. Henderson, *Journal of the Association for Laboratory Automation*, 2000, **5**, 75–78.
46 H. Inerowicz, S. Howell, F. Regnier and R. Reifenberger, *Langmuir*, 2002, **18**, 5263–5268.
47 K. Shirai, K. Mawatari and T. Kitamori, *Small*, 2014, **10**, 1514–1522.
48 J. S. Yudkin, M. Kumari, S. E. Humphries and V. Mohamed-Ali, *Atherosclerosis*, 2000, **148**, 209–214.
49 A. G. Vos, N. S. Idris, R. E. Barth, K. Klipstein-Grobusch and D. E. Grobbee, *PloS one*, 2016, **11**, e0147484.
50 I. Kushner, *Science*, 2002, **297**, 520–521.
51 P. M. Ridker, *Circulation*, 2003, **107**, 363–369.
52 S. K. Vashist, A. Venkatesh, E. M. Schneider, C. Beaudoin, P. B. Luppa and J. H. Luong, *Biotechnology advances*, 2016, **34**, 272–290.
53 A. Qureshi, Y. Gurbuz and J. H. Niazi, *Sensors and Actuators B: Chemical*, 2012, **171**, 62–76.
54 H. Shimizu, M. Kumagai, E. Mori, K. Mawatari and T. Kitamori, *Analytical Methods*, 2016, **8**, 7597–7602.
55 B. Nix and D. W. Wild, *The immunoassay handbook, 2nd Ed.*, Nature Publishing Group, New York, 2001, pp. 198–210.
56 D. A. Armbruster and T. Pry, *Clin Biochem Rev*, 2008, **29**, S49–52.
57 G. C. Allen, F. Sorbello, C. Altavilla, A. Castorina and E. Ciliberto, *Thin Solid Films*, 2005, **483**, 306–311.
58 E. T. Vandenberg, L. Bertilsson, B. Liedberg, K. Uvdal, R. Erlandsson, H. Elwing and I. Lundstr'om, *Journal of Colloid and Interface Science*, 1991, **147**, 103–118.
59 P. M. S. John and H. Craighead, *Applied physics letters*, 1996, **68**, 1022–1024.
60 N. A. Lapin and Y. J. Chabal, *The Journal of Physical Chemistry B*, 2009, **113**, 8776–8783.
61 C. Wingren and C. A. Borrebaeck, *Drug discovery today*, 2007, **12**, 813–819.
62 M. Lynch, C. Mosher, J. Huff, S. Nettikadan, J. Johnson and E. Henderson, *Proteomics*, 2004, **4**, 1695–1702.

# Microcontact printing with aminosilanes: creating biomolecule micro- and nanoarrays for multiplexed microfluidic bioassays

Shivani Sathish,‡ Sébastien G. Ricoult,‡ Kazumi Toda-Peters and Amy Q. Shen*

Micro/Bio/Nanofluidics Unit, Okinawa Institute of Science and Technology Graduate University, Okinawa, 904-0495 Japan

## Table of contents:

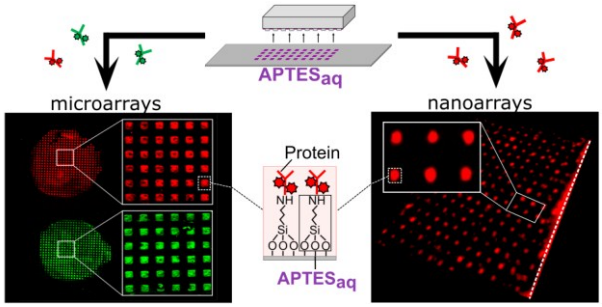


**Figure:** Aqueous based microcontact printing (μCP) to create micro- and nanoarrays of (3-aminopropyl)triethoxysilane (APTES) on glass substrates of microfluidic devices for covalent immobilization of DNA aptamers and antibodies.